Charge Recombination between $P700^+$ and A_1^- Occurs Directly to the Ground State of P700 in a Photosystem I Core Devoid of F_X, F_B, and F_A[†]

Patrick V. Warren,[‡] John H. Golbeck,*[,‡] and Joseph T. Warden*[,§]

Department of Biochemistry, University of Nebraska, Lincoln, Nebraska 68583-0718, and Department of Chemistry, Rensselaer Polytechnic Institute, Troy, New York 12180-3590

Received September 25, 1992; Revised Manuscript Received November 4, 1992

ABSTRACT: The charge recombination between $P700^+$ and electron acceptor A_1^- was studied by flash kinetic spectroscopy in a photosystem I core devoid of iron–sulfur centers F_X, F_B, and F_A. We showed previously that the majority of the flash-induced absorption change at 820 nm decayed with a 10-μs half-time, which we assigned to the disappearance of the P700 triplet formed from the backreaction of $P700^+$ with A_1^- [Warren, P. V., Parrett, K. G., Warden, J. T., & Golbeck, J. H. (1990) *Biochemistry 29*, 6545–6550]. We have reinvestigated this assignment in the near-UV, blue, and near-IR wavelength regions. The difference spectrum from 380 to 480 nm and from 720 to 910 nm shows that the $P700^+$ A_1^- charge recombination is dominated by the P700 cation rather than the P700 triplet. Accordingly, the 10-μs kinetic transient represents the direct backreaction of $P700^+$ with A_1^-, which repopulates the ground state of P700. This is unlike a P700–F_A/F_B complex where, in the presence of reduced F_X^-, F_B^-, and F_A^-, the $P700^+$ A_1^- charge recombination populates the P700 triplet state [Sétif, P., & Bottin, H. (1989) *Biochemistry 28*, 2689–2697]. The A_1 acceptor is highly susceptible to disruption by detergents in the absence of iron–sulfur center F_X. The addition of 0.1% Triton X-100 to the P700–A_1 core leads to a ~2.5-fold increase in the magnitude of the flash-induced absorption change at 780 nm; thereafter, 85% of the absorption change decays with a 25-ns half-time and 15% decays with a 3-μs half-time. The spectrum of the 25-ns phase is a convolution of contributions from both $P700^+$ and A_0^-. When the $P700^+$ spectrum is subtracted, the spectrum of A_0^- displays a maximum at 760 nm and doublet minima at 412 and 438 nm and has an extinction coefficient 1.4 and 1.8 times that of $P700^+$ at 438 and 790 nm, respectively. The spectrum of the 3-μs kinetic phase shows a broad absorption increase between 730 and 820 nm accompanied by a broad bleaching between 390 and 450 nm, consistent with the decay of the P700 triplet formed in low quantum yield from the backreaction of $P700^+$ with A_0^-. The rise time of the P700 triplet was measured to be ~25 ns, a value identical to that of the $P700^+$ A_0^- charge recombination.

There are several ways to determine the properties of the electron acceptors A_0, A_1, F_X, F_B, and F_A on the reducing side of photosystem I. One method is to chemically or photochemically reduce the particular electron acceptor, such as F_A or F_B, thereby forcing charge separation between P700 and a preceding electron acceptor, such as F_X. With this technique one can "isolate" the various electron acceptors up to and including A_0 [see Sauer et al. (1979)]. This strategy has been highly successful at uncovering the identities of the bound electron acceptors and in describing their detailed kinetic and redox properties. A second method is to remove a particular acceptor from the photosystem I complex, leaving the preceding component to serve as the terminal electron acceptor from P700. Methods are now available for the successive removal of the F_A/F_B-containing PsaC protein (Parrett et al., 1989; Hoshina et al., 1990), for the oxidative denaturation of the F_X cluster (Warren et al., 1990), and for the physical removal of the A_1 acceptor (Ikegami et al., 1989) from the photosystem I complex. This strategy has been successful in allowing the properties of an individual electron acceptor, such as F_X, to be determined in the absence of nearby acceptors, such as F_A and F_B (McDermott et al., 1989; Petrouleas et al., 1989). More recently, reconstitution protocols have been developed for A_1 (Itoh et al., 1987; Biggins & Mathis, 1988), for the F_X iron–sulfur cluster (Parrett et al., 1990), and for the F_A/F_B iron–sulfur clusters (Mehari et al., 1991). These procedures are applicable for rebinding native or genetically modified polypeptides to the P700–F_X core for detailed spectroscopic analysis (Li et al., 1991; Zhao et al., 1991).

The two methods described above might be expected to yield similar information about a particular electron acceptor, but in practive this has not been the case. Compared to that observed when an acceptor is removed from the photosystem I reaction center, the backreaction kinetics of a particular electron acceptor with $P700^+$ can be altered when a second, reduced acceptor is in close proximity (Sétif & Mathis, 1986; Golbeck & Cornelius, 1986). Furthermore, the correlation of a spectroscopic component with a specific electron acceptor can be problematic when the kinetics are influenced by the electrostatic field of a nearby reduced acceptor. This point is exemplified by the alternative identification of F_X or A_1 as the reaction partner to P700 in photosystem I complexes containing reduced F_A^- and F_B^- (Brettel, 1989; Warden, 1989). Ideally, the two methods should be used together to supply a complete description of the particular electron acceptor under study.

We reported earlier the isolation of a photosystem I core which is devoid of bound iron–sulfur clusters F_X, F_B, and F_A but in which electron flow is retained from P700 to the intermediate electron acceptor, A_1 (Warren et al., 1990). In this P700–A_1 core, the majority of the flash-induced absorption

[†] Supported by grants from the National Science Foundation [DMB-904333 (J.H.G.)] and the National Institutes of Health [GM26133 (J.T.W.)].

* Authors to whom correspondence should be addressed.

[‡] University of Nebraska.

[§] Rensselaer Polytechnic Institute.

0006-2960/93/0432-849$04.00/0

change at 820 nm decays with a 10-μs half-time, which we interpreted as the disappearance of the P700 triplet formed from the backreaction of $P700^+$ with A_1^-. This assignment was based on the temporal similarity to a 4–5-μs kinetic phase observed in a photosystem I complex where F_X, F_B, and F_A were reduced prior to illumination (Sétif & Bottin, 1989). An additional 750-ns kinetic phase was described [later more accurately measured as 250 ns (Sétif & Brettel, 1990)] and was proposed to correspond to the recombination between $P700^+$ and A_1^-, which concomitantly populates the triplet state of P700 with a quantum yield close to 1.0. Although the 10-μs kinetic phase in our P700–A_1 core was similar to the 4–5-μs relaxation of the P700 triplet, we did not observe the 250-ns phase that should have resulted from the $P700^+$ A_1^- charge recombination process. In this paper, we detail the spectral and kinetic properties of various photosystem I subthylakoid preparations in the near-UV,[1] blue, and near-IR wavelength regions. We report a qualitative difference in the behavior of the $P700^+$ A_1^- charge recombination in the absence of F_X, F_B, and F_A relative to that found when the bound iron–sulfur clusters are present and prereduced. Our results show that the $P700^+$ A_1^- backreaction proceeds directly to the ground state of P700 in a photosystem I core devoid of iron–sulfur clusters F_X, F_B, and F_A.

MATERIALS AND METHODS

Subchloroplast Preparations. Most of the photosystem I core preparations described here are stripped of cofactors rather than polypeptides; hence, we refer to the depleted preparations by the terminal electron acceptor present. Hence, the "native photosystem I complex" is named the P700–F_A/F_B complex, the "photosystem I core protein" (Parrett et al., 1989) is the P700–F_X core, and the "apo-F_X particle" (Warren et al., 1990) is the P700–A_1 core. The P700–A_0 (Triton) core is a new preparation which is stripped of A_1, F_X, F_B, and F_A but which retains 110 Chl/P700. The P700–F_A/F_B complex and the P700–F_X core were prepared from *Synechococcus* sp. PCC 6301 thylakoids according to the method of Parrett et al. (1989). The P700–A_1 core was isolated from the P700–F_X core by treatment with 3 M urea and 5 mM $K_3Fe(CN)_6$ at 20 °C according to the method of Warren et al. (1990). The P700–F_X core was stripped of excess detergent by sucrose density ultracentrifugation in a Triton-free, 0.1–1 M sucrose gradient containing 50 mM Tris, pH 8.3, prior to treatment. Replicate isolations of the P700–A_1 core were prepared independently at the University of Nebraska and Rensselaer Polytechnic Institute. Both preparations exhibited similar kinetic and redox properties. The P700–A_0 (Triton) core was prepared by treating the P700–A_1 core for 2 h with 0.1% Triton X-100 at a chlorophyll concentration of 100 μg/mL. Similarly, the P700–A_0 (SDS) core was produced by treating the P700–F_A/F_B complex for 2 h with 1% SDS at a chlorophyll concentration of 100 μg/mL. Both of these detergent-treated samples were purified by ultracentrifugation at 113000*g* (SW-27 rotor) in a detergent-free, 0.1–1.0 M sucrose density gradient containing 50 mM Tris buffer at pH 8.3. The P700–A_0 (Triton) and P700–A_0 (SDS) cores banded about halfway down the gradient after 18 h of centrifugation. All photosystem I preparations were concentrated to 1 mg Chl/mL by ultrafiltration and stored in 20% glycerol at −80 °C.

Chlorophyll a Preparation. Chlorophyll *a* was extracted from *Synechococcus* sp. PCC 6301 (*Anacystis nidlans* TX-20) membrane fragments with two portions of dry diethyl ether. The pigments were solvent-exchanged into petroleum ether containing 0.5% 1-propanol and purified over a powdered sugar column (Strain & Svec, 1966). The spectrally pure chlorophyll *a* was exchanged into either cyclohexanol containing 2% ethanol or 2% Triton X-100 micelles for kinetic analysis.

Spectroscopic Measurements. Transient absorbance changes between 720 and 910 nm in the nano- and microsecond time domain were measured with a laboratory-built double-beam spectrometer. The measuring beam was provided by a Schwartz Electro-Optics titanium–sapphire laser (Model TI-SPB) operated in the standing wave configuration and pumped by a CW argon-ion laser (Spectra-Physics Model 2020-05). Using 3.8 W of pump power (all lines), the titanium–sapphire laser could be tuned continuously from 720 and 920 nm (with two overlapping mirror sets) at a wavelength-dependent beam intensity of 100–250 mW. Due to temporal instability (the argon-ion laser is noisy on the time scale of the measurement), the beam from the titanium–sapphire leaser was split; the reference beam was passed directly to a planar diffused silicon photodiode detector (PIN-10D, reverse biased to 30 V), and the sample beam was passed through the cuvette and detected by a second photodiode. The sample detector was located 3 m distant from the cuvette to eliminate the flash artifact from the laser and the fluorescence from the sample. The intensity of the measuring beam was adjusted using a variable metallic beam splitter/attenuator to provide 50 mW of incident radiation at the sample photodiode; the intensity of the reference beam was matched using a second beam splitter/attenuator. For nanosecond time resolution, two transimpedance amplifiers (UDT Model 700, 400-MHz bandwidth and reverse biased to 30 V) were used to convert the photocurrent into a voltage. The 10-ns rise time of the spectrometer was limited by the response time of the PIN-10D silicon photodiodes; the low-frequency roll-off of the transimpedance amplifiers restricted data collection to 500 ns. For microsecond time resolution, a 500 Ω resistor was used to convert the photocurrent into a voltage, and a preamplifier (EG&G Model 115) provided a 10-fold voltage gain and limited the bandwidth to 70 MHz. In both nano- and microsecond time ranges, the analog signals derived from the sample and reference beams were subtracted and amplified using a DC-coupled differential comparator (Tektronix Model 11A33, 150-MHz bandwidth) and digitized with a Tektronix DSA 601 oscilloscope. The data were ported to a Macintosh IIci computer using software developed in-house. Curve-fitting and data analysis were performed using a commercial software package (IGOR, WaveMetrics). The sample was excited at 337.1 nm using a 2.3 MW nitrogen laser (PTI Model PL2300, 1.4 mJ and 600-ps pulsewidth) operated at a frequency of 1 Hz. The samples contained 50 (nanosecond time scale) or 100 μg/mL Chl (microsecond time scale) in a 1-cm path length cuvette containing 0.1 mM DCPIP and 5 mM ascorbate in 100 mM Tris (pH 8.3).

Transient optical absorbance changes between 380 and 480 nm were measured in the microsecond time domain with a single-beam spectrophotometer comprised of a 300 W Eimac xenon-arc monitoring source and a 200-mm monochromator (Photon Technology International). An EMI Model 9816 photomultiplier was utilized to detect the optical transients. Using a 600-Ω load reistor, the minimum instrumental response time ($t_{1/2}$) was 60 ns. For studies of the microsecond time range, a preamplifier (EG&G Model 113) was inserted between the photomultiplier and the digitizer to provide gain

[1] Abbreviations: UV, ultraviolet; IR, infrared; Chl, chlorophyll; SDS, sodium dodecyl sulfate; CP1, chlorophyll protein 1; DCPIP, 2,6-dichlorophenolindophenol; ESR, electron spin resonance; Tris, tris-(hydroxymethyl)aminomethane; AIMS, aminoiminomethanesulfinic acid.

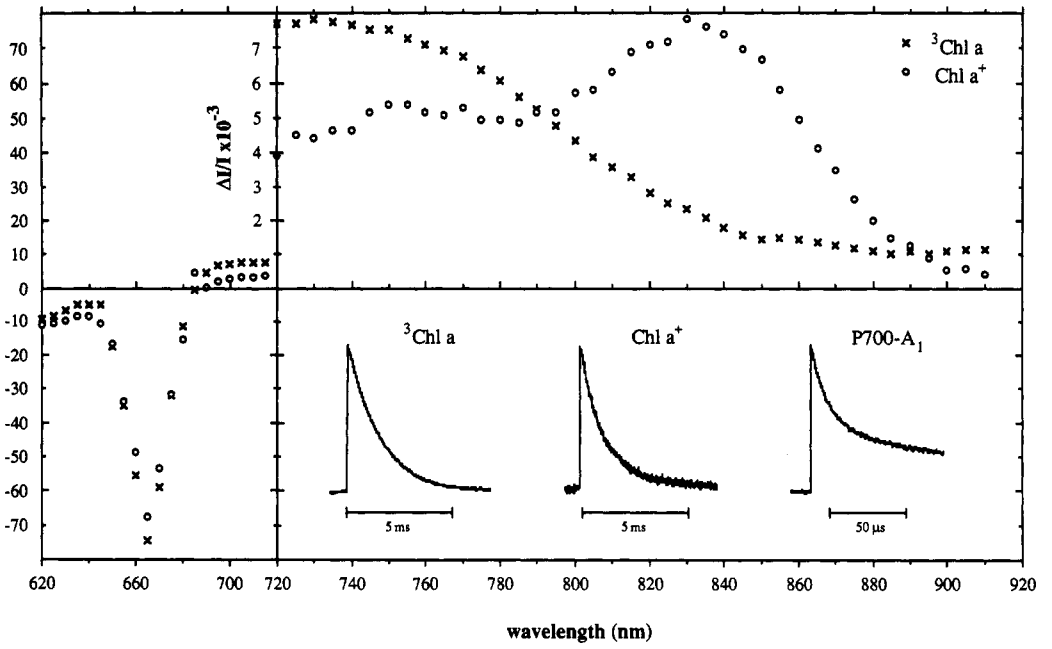

FIGURE 1: Flash-induced, point-by-point difference spectra of the chlorophyll *a* triplet (^{3}Chl *a*) and chlorophyll *a* cation (Chl *a*$^+$). The difference spectra of ^{3}Chl *a* (crosses) and Chl *a*$^+$ (open circles) were obtained by dissolving purified chlorophyll *a* to a concentration of 5 µg/mL in cyclohexanol containing 2.0% ethanol. The Chl *a*$^+$ was generated by addition of benzoquinone to a final concentration of 1 mM. The ^{3}Chl *a* and Chl *a*$^+$ spectra were normalized to the P700$^+$ spectrum at points of maximum ΔOD. The flash-induced absorption changes of the Chl *a* triplet and Chl *a*$^+$ were determined in the visible using a single-beam spectrometer capable of microsecond time resolution (Parrett et al., 1989). The measurements in the near-IR were performed using the collimated measuring beam provided by a titanium–sapphire laser. The kinetics of the flash-induced absorption transients in the ^{3}Chl *a*, the Chl *a*$^+$, and the P700–A$_1$ core are shown in the lower half.

while limiting the electrical bandwidth to 300 kHz. Bandpass filters (Mashpriborintorg SS-4, SZS-21, and FS-6) were placed in front of the detector to reject fluorescence or scattered laser light. To minimize exposure of the sample to the actinic and monitoring beams, shutters were installed in both beam paths and were programmed to be open (typically 4 ms) coincident with the laser flash. A LeCroy 9410 digital oscilloscope, controlled by a Zenith 80386 microcomputer, was used for data collection. Near-UV and blue optical transients in the nanosecond time domain were measured at room temperature with a purpose-designed flash photolysis instrument that utilized for a monitoring source an EG&G FX200U UV-grade bulb flashlamp, powered by a 15-J supply. The image of the arc of the flashlamp was focused behind the sample cell onto a 2.0-mm slit to minimize fluorescence, and the resulting image was collected and refocused onto the entrance slit of a 250-mm monochromator (Jarrell-Ash). An EMI Model 9816 photomultiplier was utilized to detect the optical transients; the minimum instrumental response time ($t_{1/2}$) was 5 ns. A Tektronix 7912AD programmable digitizer, which was controlled by an 80286-based microcomputer, was used for data collection. Timing for both the detecting flash and the data collection trigger to the Tektronix recorder was controlled by a SRS DG535 pulse generator. Software routines for collecting data from the nanosecond optical spectrometer were derived from the Tektronix Guru II package. The bandwidth of the monochromators in both the micro- and nanosecond flash spectrometer configurations was between 0.9 and 3.6 nm. Kinetic analysis of the experimental data was performed either with a Sun IPC workstation, using xvgr (P. J. Turner, Oregon Graduate Institute), or with a Macintosh II, using the IGOR graphing and analysis package. Actinic illumination (0.5–1 mJ, 600 nm, 0.47 Hz) was provided by a TDL 51 dye laser that was pumped by the 532-nm harmonic of a TG 581C Nd–YAG laser (both lasers by Continuum). The samples contained 10–25 µg/mL Chl, 50 µM DCPIP, and 2 mg/mL dithiothreitol in a 50 mM Tris buffer (pH 8.3) in a 1-cm path length cuvette. For construction of the P700$^+$ spectrum in the P700–F$_X$ core, 2 mM methylviologen was added to eliminate the contribution of F$_X^-$. For construction of the difference spectra in Figures 2 and 3, the amplitude of the transient change in absorbance was determined at each wavelength by extrapolation of the decay kinetics to the incidence of the actinic flash. To compensate for any aggregation or long-term aging effects in the sample, the magnitude of each trace was normalized against the level of the 430- (difference spectra in the blue) and 820-nm transients (difference spectra in the red and near-IR), which were monitored periodically over the course of the experiments.

RESULTS

Spectrum of P700$^+$ A$_1^-$ in the Near-IR and UV–Blue. A chlorophyll *a* cation can be distinguished from a chlorophyll *a* triplet in the near-IR and blue regions of the spectrum (Mathis & Sétif, 1981). To determine the origin of the 10-µs kinetic phase in the P700–A$_1$ core, we compared the flash-induced difference spectrum with that of a chlorophyll *a* cation and a chlorophyll *a* triplet, both generated in degassed cyclohexanol. When measured at 740 nm, the chlorophyll *a* triplet decays monotonically with a half-time of 1.5 ms following a laser flash (Figure 1, lower left). The point-by-point difference spectrum (crosses, Figure 1) shows a sharp absorption minimum at 665 nm, followed by an absorption increase which peaks at 730 nm and a shallow decline from 760 to 840 nm (a similar spectrum was measured for chlorophyll *a* dissolved in 2% Triton X-100 micelles except that the half-time for the triplet decay was 200 µs). In the presence of an electron acceptor such as benzoquinone, a chlorophyll *a* cation can be produced with a quantum yield between 0.6 and 0.8 (Hurley et al., 1980). When monitored at 820 nm, the chlorophyll *a* cation decays monotonically with a half-time of about 1.1 ms following a laser flash (Figure 1, lower center). The point-by-point difference spectrum (Figure 1, open circles) shows a sharp absorption decrease at

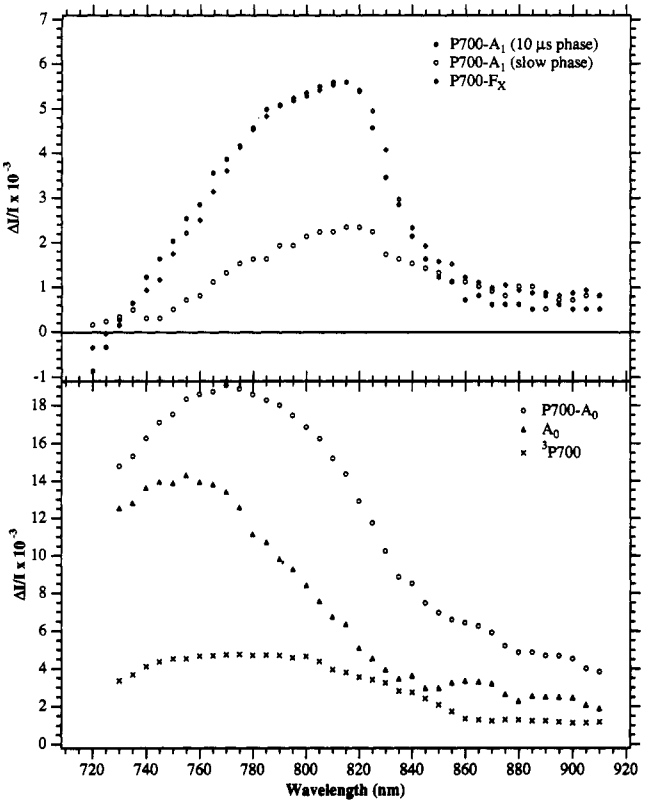

FIGURE 2: (Top) Point-by-point difference spectra between 720 and 910 nm of the 10-μs component (solid circles) and the minority slow kinetic component in the P700–A_1 core (open circles) and $P700^+$ (open diamonds) in the P700–F_X core. (Bottom) Point-by-point difference spectra between 730 and 910 nm for $P700^+$–A_0^- (open circles), A_0^- (triangles), and P700 triplet (crosses) in the P700–A_0 (Triton) core. The difference spectra of the P700–A_1 and P700–F_X cores were obtained directly from flash-induced absorption changes on a microsecond timescale. The P700–F_X spectrum was normalized to the P700–A_1 spectrum at 815 nm to allow comparison between the two photosystem I cores. The difference spectrum of A_0^- was determined by subtracting the $P700^+$ from the composite absorption change at the onset of the flash. The difference spectrum of the P700 triplet was determined by extrapolating the absorption change related to the slow kinetic phase at the onset of the flash. All measurements were performed at 50 μg/mL Chl in 50 mM Tris buffer (pH 8.3) containing 100 μM DCPIP and 5 mM sodium ascorbate.

665 nm, followed by a broad absorption increase that remains relatively flat between 720 and 790 nm, followed by a peak 830 nm and a relatively steep decline between 840 and 900 nm. The enhanced absorption between 720 and 790 nm probably represents a contribution from the residual chlorophyll *a* triplet.

In the P700–A_1 core devoid of iron–sulfur centers F_X, F_B, and F_A, the flash-induced absorption change at 820 nm decays with two major kinetic phases: 62% of the transient decays with a half-time of 10 μs and 38% decays more slowly, with a half-time >250 μs (Figure 1, inset right). The point-by-point difference spectrum of the 10-μs component (Figure 2 top, solid circles) indicates a rising total absorption change between 720 and 770 nm followed by a leveling off at 780 nm, a broad peak centered at 815 nm, and a rapid decline after 820 nm. This spectrum is unlike that of a chlorophyll *a* triplet but rather resembles closely that of a chlorophyll *a* cation (cf. Figure 1). The slow kinetic phase has a similar spectrum (Figure 2 top, open circles), indicating that this absorption change also represents the P700 cation (there may be several kinetic phases present, including a minor contribution by a component that has an enhanced absorption change at wavelengths >860 nm). While the 10-μs phase most likely represents charge recombination between $P700^+$ and A_1^-, the identity of the slow kinetic phase is unclear. It does not represent unreacted P700–F_X core since, within the limits of the ESR-based measurement, the P700–A_1 core contains no more than 10% F_X. We suspect that the slow kinetic phase represents a further manifestation of the $P700^+$ A_1^- back-reaction.

A potential weakness of the above comparison is that both the triplet and cation spectra of chlorophyll *a* in organic solvent or detergent could differ significantly from that of P700, a protein-bound chlorophyll *a* dimer. Indeed, the spectrum of the putative P700 cation in the P700–A_1 preparation appears to be blue-shifted 20 nm relative to that of the chlorophyll *a* cation measured in organic solvent (cf. Figures 1 and 2). We therefore measured the flash-induced difference spectrum of $P700^+$ in a P700–F_X core from *Synechococcus* sp. PCC 6301, where the majority of the charge recombination from F_X^- is known to result in the formation of $P700^+$ (Parrett et al., 1989). The point-by-point difference spectrum of the P700–F_X core between 720 and 910 nm is shown in Figure 2 (top, open diamonds). The P700–F_X spectrum was normalized to the P700–A_1 spectrum at 815 nm to allow comparison between the two photosystem I cores. The near-identical spectral properties of the P700–F_X and P700–A_1 cores in the near-IR constitute further evidence for the presence of a $P700^+$ cation in the latter preparation.

Complementary experiments were performed in the wavelength range 380–480 nm. The 10-μs half-time for the decay of the majority of the absorption transient is invariant of the wavelength in this region and is consistent with that observed in the near-IR. The point-by-point difference spectrum for the 10-μs transient component (Figure 3 top, solid circles) is characterized by a major bleaching at 432 nm, a minor absorption feature between 390 and 400 nm, and a rising absorption above 460 nm. Although the data were taken with a bandwidth limitation of 300 kHz, the spectrum was determined at the minimum instrumental time constant of 60 ns to check for the presence of any additional kinetic phases. No differences were observed between minimum and maximum bandwidth-limited conditions. When reexamined with an instrument capable of 5-ns time resolution, the absorption transient exhibited an instrument-limited rise time and decayed in a biphasic manner, with a minor phase (10–30%, depending on preparation) possessing a ~20-ns half-time. The relative magnitude of the nanosecond kinetic phase compared to the total absorption change is dependent on wavelength, with a more pronounced contribution at 430 and 460 nm. This kinetic phase represents charge recombination between $P700^+$ and A_0^- in slightly damaged P700–A_1 cores.

Of particular interest is the observation that the absorption change is positive in the region between 370 and 400 nm, in contrast to that reported for the chlorophyll *a* triplet (Hurley et al., 1980; den Blanken & Hoff, 1983). To evaluate the participation of a chlorophyll *a* triplet in the 10-μs absorption change, a flash-induced difference spectrum was constructed for chlorophyll *a* suspended in 2% Triton X-100 (Figure 3 top, crosses). When measured at 430 nm, the chlorophyll *a* triplet decays monotonically with a half-time of 200 μs (not shown), which is significantly faster than the 1.5-ms half-time in cyclohexanol. The observed difference spectrum of the chlorophyll *a* triplet is consistent with that reported by Hurley et al. (1980), namely a negative contribution below 400 nm, a significant bleaching between 410 and 430 nm, and a positive band above 450 nm. Hence, consistent with the

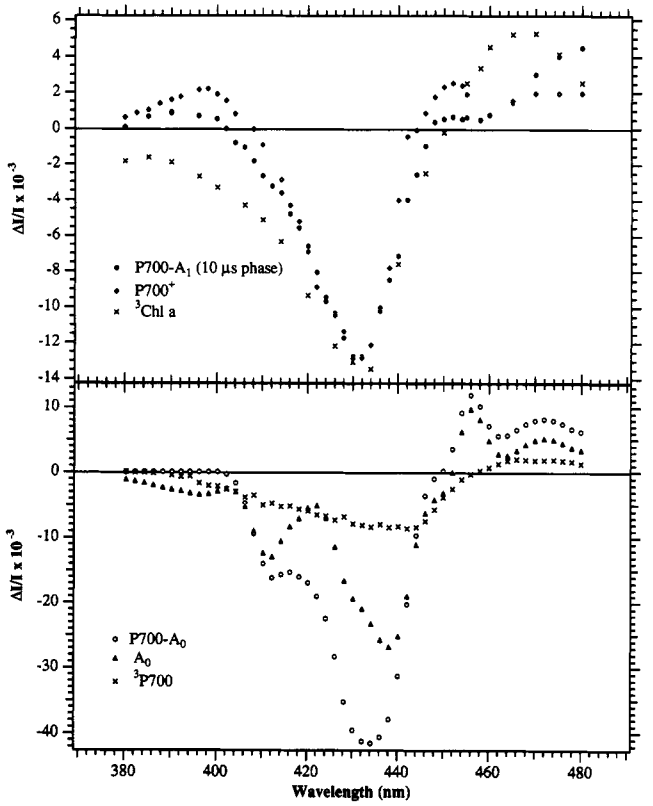

FIGURE 3: (Top) Point-by-point difference spectra between 380 and 480 nm of ^{3}Chl *a* in Triton X-100 (crosses), P700–A_1 core (solid circles), and $P700^+$ (open diamonds) in the P700–F_X core. (Bottom) Point-by-point difference spectra between 380 and 480 nm for $P700^+$–A_0^- (open circles), A_0^- (triangles), and P700 triplet (crosses) in the P700–A_0 (Triton) core. The difference spectrum of the P700–A_1 core was determined from kinetic experiments in the microsecond time domain. The $P700^+$ difference spectrum was constructed from transient kinetics in the microsecond time domain in the P700–F_X core. The $P700^+$ difference spectrum was normalized to the P700–A_1 spectrum at 435 nm to allow comparison between the two photosystem I cores. The difference spectrum of A_0^- was obtained by subtracting the concentration-normalized spectrum of $P700^+$ from the $P700^+$–A_0^- composite spectrum in the nanosecond time domain. All measurements were performed at 22 μg/mL Chl in 50 mM Tris buffer (pH 8.3) containing 50 μM DCPIP, 2 mg/mL dithiothreitol, and 2 mM methylviologen.

observations presented in Figure 2 for the near-IR, the difference spectrum for the 10-μs $P700^+$ A_1^- charge recombination is incompatible with an assignment as a chlorophyll triplet. This assertion is confirmed in Figure 3 (top) in which the difference spectrum between 380 and 480 nm is presented for the $P700^+$ cation in the P700–F_X core (open diamonds). In this experiment, 2 mM methylviologen was added to eliminate the contribution from F_X^- in this wavelength region [see Parrett et al. (1989)]. The $P700^+$ difference spectrum was normalized to the P700–A_1 spectrum at 435 nm to allow comparison between the two photosystem I cores. The principal bleaching in the P700–F_X core is centered at 432 nm and is superimposable on the bleaching assigned to $P700^+$ in the P700–A_1 core. The observed experimental variances between the two samples, notably in the wavelength regions below 400 nm and greater than 450 nm, most probably reflect contributions from the A_1 acceptor and electrochromic shifts due to a nearby carotenoid [see Brettel (1989)]. The detailed spectrum of A_1^- in the near-UV/blue region will be reported separately (K. Brettel and J. H. Golbeck, unpublished results). Similarly, the spectrum of the slow kinetic phase (data not shown) resembles that of the P700 cation.

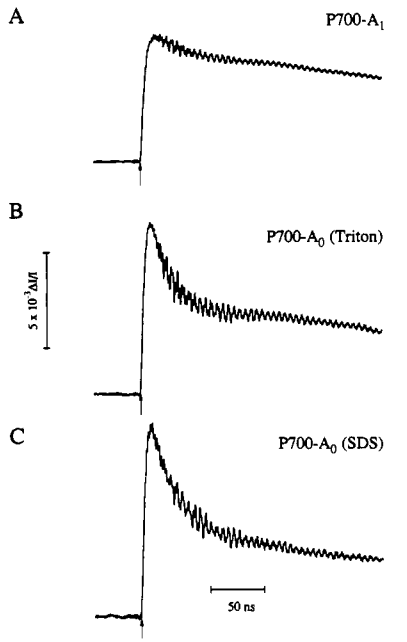

FIGURE 4: Flash-induced absorption change at 820 nm on the nanosecond time scale of the (A) P700–A_1 core prepared by oxidative denaturation of the iron–sulfur cluster in the P700–F_X core, (B) the P700–A_0 core prepared with 0.1% Triton X-100 (TX-100), and (C) the P700–A_0 core prepared with SDS. All measurements were performed at 50 μg/mL Chl in 50 mM Tris buffer containing 0.1 mM DCPIP and 5 mM sodium ascorbate.

Functional Displacement of A_1 with Triton X-100. During the course of these studies, we found that the addition of 0.1% Triton X-100 leads to a gradual replacement of the 10-μs kinetic component with a 25-ns kinetic component followed by a minor, 3-μs, decay (Figure 4A,B). The half-time for the Triton-mediated onset of the 25-ns kinetic phase is about 10 min at 20 °C. This result implies that a detergent as mild as Triton X-100 has the ability to disrupt the function of A_1, thereby effecting charge separation and recombination between the primary reactants $P700^+$ and A_0^-. The attempted removal of excess Triton X-100 by ultracentrifugation in a detergent-free sucrose gradient did not result in the restoration of A_1 function. Further, the addition of 0.1–1% Triton X-100 to the more intact P700–F_X core did not induce a similar onset of the 25-ns kinetic phase. We suggest that removal of F_X may provide the detergent access to the A_1 binding site, resulting in its disruption and/or solubilization of the A_1 acceptor. An additional approach for spectroscopic study of the P700–A_1 core exploits the propensity of A_1 to become doubly reduced in the presence of a strong reductant. As previously reported (Warren et al., 1990), treatment of the P700–A_1 core with AIMS at pH 10 abolishes the 10-μs decay kinetics and induces biphasic kinetics comprised of a major ca. 25-ns decay component and a minor 3-μs component. These kinetics are similar to the 35-ns $P700^+$ A_0^- recombination half-time observed in a photosystem I particle where phylloquinone had been extracted with diethyl ether (Mathis et al., 1988).

Spectrum of $P700^+$ A_0^- after Functional Displacement of A_1. To verify this assignment, the point-by-point difference spectrum of the 25-ns component was constructed in the P700–A_0 (Triton) core. The data (Figure 2 bottom, open circles) show a large absorption increase between 720 and 800 nm, peaking at 770 nm, and a shallow decline to 840 nm. Since this absorption transient represents contributions from the photosystem I donor–acceptor pair, the spectrum of $P700^+$ was subtracted to yield only the spectrum of the acceptor. The

latter (open triangles) is compatible with the spectrum of A_0^-, showing a peak at about 750 nm, followed by a rather steep decline, leveling off at 830 nm. The extinction coefficient of the A_0 anion appears to be larger than that of the P700 cation by a factor of 1.8 at 790 nm and also is consistent with that reported by Mathis et al. (1988). The point-by-point difference spectrum of the 3-μs component shows a modest absorbance increase at 730 nm, remaining flat from 740 to 800 nm and declining gradually to about 860 nm (Figure 2 bottom, crosses). Beyond 860 nm, the absorbance remains relatively constant to wavelengths of at least 910 nm. Except for a 30-nm red shift, this spectrum closely resembles that of a chlorophyll *a* triplet in organic solvent (cf. Figure 1). This difference spectrum can therefore be assigned to the P700 triplet, derived in low-yield from $P700^+$ A_0^- charge recombination (Sétif & Brettel, 1990). This spectrum is clearly unlike that of the 10-μs kinetic component or the slow kinetic component of the P700–A_1 core (cf. Figure 2).

The point-by-point difference spectrum of the 25-ns component in the region 380–480 nm (Figure 3 bottom, open circles) is characterized by a strong bleaching centered at 435 nm with a prominent shoulder expressed at ca. 415 nm. An additional absorption peak occurs above 450 nm. The approach applied previously is utilized to obtain the spectrum of A_0^-. The spectrum of A_0^- (open triangles) displays a wealth of features, the most notable being the doublet bleaching with minima at 412 and 438 nm. The extinction coefficient of A_0^- determined at the 438 minima is 63 500, a value 1.4 times that of $P700^+$ measured at 430 nm (45 000). The spectrum of the P700 triplet derived from the $P700^+$ A_0^- recombination process is also presented in Figure 3 (bottom, crosses). The spectrum of this species is characterized principally by a broad bleaching that extends between ca. 390 and 445 nm with a minimum in the vicinity 435–440 nm. Positive absorption features are observed below 360 nm (data not shown) and above 450 nm. This difference spectrum for the P700 triplet in the near-UV and blue resembles closely that presented for the chlorophyll *a* triplet in detergent (Figure 3 top) and is thus not congruent with that presented for the 10-μs transient in the P700–A_1 core. We obtained the same spectrum of $P700^+$ A_0^- in the near-IR and blue regions in a P700–A_1 core when the electron acceptor A_1 was reduced with AIMS at pH 10 prior to analysis (not shown).

Rise Time of the $P700^+$ A_1^- Recombination. One corollary of the above hypothesis is that the P700 triplet derived from the recombination between $P700^+$ and A_1^- should demonstrate a rise time of 250 ns (Sétif & Brettel, 1990), a process which should be observable at appropriate wavelengths in the near-IR, visible, and near-UV regions. The spectral analysis discussed above showed that 730 and 430 nm are particularly suitable wavelengths to study the formation of the P700 triplet. We therefore compared the rise times of the flash-induced absorption change at these wavelengths in the P700–A_1 core and in the P700–A_0 (Triton) core. As shown in Figure 5A, the flash-induced absorption change in the P700–A_1 core shows an absorption increase at 730 nm with a rise time clearly instrument-limited to <10 ns. The backreaction is biphasic: about 10% of the sample decays with a 25-ns half-time, and 90% decays with 10-μs and longer kinetic phases (not resolved here due to the low-frequency roll-off of the transimpedance amplifier). The 25-ns phase most likely represents the $P700^+$ A_0^- charge recombination in damaged reaction centers, where the complete denaturation of F_X results in the inactivation of a small percentage of A_1. The amplitude of the 25-ns phase is overrepresented due to the greater contribution of the A_0^-

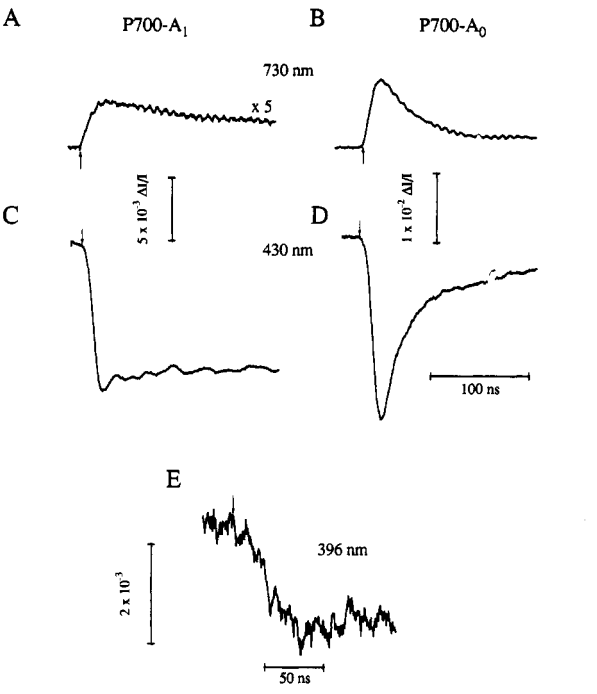

FIGURE 5: Flash-induced absorption transients of the P700–A_1 core (A, C) and the P700–A_0 (Triton) core (B, D, E). Spectra were determined at 730 (A, B), 430 (D, C), and 396 nm (E). The P700–A_1 core was prepared by oxidative denaturation of the P700–F_X core with 3 M urea and 5 mM potassium ferricyanide. The P700–A_0 (Triton) core was prepared by treating the P700–A_1 core with 0.1% Triton X-100. (A) and (B) were performed at 50 μg/mL Chl in 50 mM Tris buffer (pH 8.3) containing 5 mM sodium ascorbate and 100 μM DCPIP. (C–E) were performed at 22 μg/mL Chl in buffer in 50 mM Tris (pH 8.3) containing 2 mg/mL dithiothreitol and 50 μM DCPIP.

anion at this wavelength (for comparison at 820 nm, see Figure 2). When corrected for the contribution of A_0^-, only a very small percentage of the total absorption change in the P700–A_1 core is represented by the $P700^+$ A_0^- charge-separated pair. Given that >90% of the absorption change is due to the P700–A_1 component, there is no indication of a rise time slower than 10 ns. The backreaction kinetics in a P700–A_0 (Triton) core (Figure 5B), measured at the same chlorophyll concentration, is dominated by the 25-ns backreaction. When extrapolated to the onset of the flash, the overall absorption change is due largely to A_0^- and is nearly 10-fold that seen in the P700–A_1 core. The rise time of the absorption change in the P700–A_0 (Triton) core is instrument-limited (<10 ns).

A complementary examination of the formation kinetics for the P700–A_1 core and the P700–A_0 (Triton) core were performed over the 380–480-nm wavelength range. Particular emphasis was expended at wavelengths in the vicinity of 390–400 and 450–460 nm, since the relative contribution of the P700 triplet is enhanced in these regions. At 430 nm (Figure 5C) the transient absorption for the P700–A_1 pair exhibits a wavelength-invariant rise time which is instrument-limited ($t_{10-90} \sim 9$ ns). Similar studies with the P700–A_0 (Triton) core (Figure 5D) demonstrated similar instrument-limited rise times for the $P700^+$–A_0^- pair. Indeed, at all wavelengths studied between 350 and 480 nm and between 730 and 900 nm, the kinetics are consistent with that expected from the relative contributions of the amount of P700–A_1 and P700–A_0, and in no instance was the rise time slower than 10 ns except that attributed to the formation of the P700 triplet from the $P700^+$–A_0^- precursor (see below).

Rise Time of the P700 Triplet Derived from the $P700^+$ A_0^- Recombination. Close scrutiny of the spectrum in Figure 3B

(bottom) reveals that in the 390–400-nm window the formation of the P700 triplet can be monitored without interference from the $P700^+ A_0^-$ pair. This observation permits the kinetics of the formation of the P700 triplet to be determined unequivocally. The kinetics for the formation of the P700 triplet at 396 nm are presented in Figure 5E. Inspection of this trace suggests that the bleaching at 396 nm occurs concomitantly with the decay of $P700^+$ as monitored at 360 (not shown) and 430 nm (Figure 5D). An analysis of the bleaching kinetics for replicates of this trace yields a ca. 20-ns half-time for the formation of the P700 triplet, a value indistinguishable within experimental error with that observed for the $P700^+ A_0^-$ charge recombination.

DISCUSSION

A difficult issue in photosystem I research has been the identification and correlation of the spectroscopic A_1 acceptor with one of the two molecules of phylloquinone associated with the PsaA/PsaB heterodimer. After much accumulated evidence, the experimental data suggest that many (but certainly not all) of the spectroscopic signals attributed to A_1 are consistent with those characteristic of a phylloquinone anion radical. In a P700–A_1 core devoid of the F_X, F_B, and F_A iron–sulfur clusters, the identification of A_1 as the functional electron acceptor was based on the similarity of the 10-μs optical transient with the 4–5-μs half-time observed in a preparation in which F_X, F_B, and F_A were reduced prior to illumination (Sétif & Bottin, 1989; Sétif & Brettel, 1990) and additionally the transition to a 25-ns transient derived from the presumed $P700^+ A_0^-$ charge recombination after addition of AIMS at pH 10. The latter observation would be expected if A_1 were a quinone that could undergo double reduction after addition of a suitable reductant at high pH values. Further evidence that the electron acceptor under study is located between A_0 and F_X is given by the fact that it functions after the oxidative denaturation of F_X; the spin-polarized ESR signal that is a signature for the function of A_1 is present in this preparation (J. Franke and J. T. Warden, unpublished results); when the acceptor is inactivated with Triton X-100 or SDS, the $P700^+ A_0^-$ primary charge separation is observed with the concurrent loss of the spin-polarized signal.

The destruction of the A_1 acceptor with Triton X-100 resembles that of the effect of SDS on a photosystem I complex. A strong ionic detergent will destroy the function of A_1 and deplete these preparations of most, if not all, of the low molecular mass polypeptides from the PsaA/PsaB heterodimer, leaving the P700–A_0 charge separation intact. Although two molecules of phylloquinone still remain associated with the PsaA/PsaB heterodimer (Schoeder & Lockau, 1986), the A_1 acceptor is photochemically inactive. The most likely explanation for the Triton effect is that phylloquinone is dislocated within its binding site but yet bound within a hydrophobic domain on the photosystem I heterodimer. An analogous disfunction of A_1, while preserving phylloquinone content, was observed also in spinach photosystem I preparations inactivated by oxidative denaturation of the P700–F_X core with urea/ferricyanide in the presence of 1% Triton X-100 (Warden & Golbeck, 1987). The only other method to remove the phylloquinone is solvent extraction with dry diethyl ether (Ikegami et al., 1987) or methanol/hexane (Biggins & Mathis, 1988), but organic solvents also remove the β-carotene and about half of the antenna chlorophyll *a* from the reaction center. Since there is no loss of pigments from the Triton X-100-treated P700–A_1 core, this method represents an attractive alternative to organic solvent extraction (Biggins & Mathis, 1988; Ikegami et al., 1987) and SDS treatment (Figure 4C) (Brettel & Sétif, 1987) to remove the function of the A_1 electron acceptor in photosystem I.

One corollary of the above interpretation is that if A_1 is undamaged after the oxidative denaturation of F_X, it should be possible to rebuild the iron–sulfur cluster and restore electron flow to F_X. Indeed, we showed that the F_X iron–sulfur cluster could be reconstituted in the P700–A_1 core by adding β-mercaptoethanol, $FeCl_3$, and Na_2S under anaerobic conditions (Parrett et al., 1989). The flash-induced absorption change indicated nearly complete restoration of the 1.2-ms optical transient characteristic of the $P700^+ F_X^-$ backreaction, and ESR studies showed the light-induced spectrum of $P700^+ F_X^-$. The elimination of either the $FeCl_3$ or Na_2S led to only a small (ca. 15%) increase in the amount of the 1.2-ms kinetic component. However, the addition of β-mercaptoethanol, $FeCl_3$, and Na_2S under anaerobic conditions to the P700–A_0 (Triton) core did not result in any change from the dominant 25-ns backreaction between $P700^+$ and A_0^-. This would be expected if the reconstitution protocol does not restore the function of A_1 and, by inference, phylloquinone in photosystem I. The data are therefore fully consistent with the proposal that the A_1 acceptor is required for restoration of room temperature electron flow from A_0 to F_X.

One complication in the study of A_1 is that its kinetic and spectroscopic properties are usually determined by blocking electron flow to the next electron acceptor, F_X. This is done by chemically or photochemically reducing the iron–sulfur clusters, thereby forcing A_1^- to backreact with $P700^+$. The difference spectrum of A_1^-/A_1 measured in *Synechococcus* sp. (thermophilic species) under conditions of reduced F_A^- and F_B^- is consistent with the reduction of a quinone to a semiquinone anion radical (Brettel, 1989). Photoaccumulation of F_X^-, F_B^-, and F_A^- has also been shown to influence the backreaction time of A_1 with $P700^+$. For example, at 10 K, the backreaction from A_1^- to $P700^+$ in a *Synechocystis* sp. PCC 6803 photosystem I complex undergoes an acceleration from 220 to 20 μs in the presence of F_X^- (Sétif & Bottin, 1989). Earlier, a 30-μs backreaction was observed at room temperature under conditions that involved the rapid donation of a bound molecule of plastocyanin to $P700^+$ under a regime of closely spaced, repetitive flashes. This kinetic phase was attributed to the backreaction of an acceptor more primary than F_X (presumably A_1^-) with $P700^+$ (Bottin et al., 1987). Indeed, the room temperature properties of the $P700^+ A_1^-$ backreaction in the presence of F_X^-, F_B^-, and F_A^- remained uncharacterized until recently, when Sétif and co-workers (Sétif & Bottin, 1989; Sétif & Brettel, 1990) found that the P700 triplet was formed in high quantum yield from the $P700^+ A_1^-$ backreaction.

The investigations detailed here advance the premise that the redox state of an electron carrier can influence profoundly the energetics of electron-transfer events on adjacent redox intermediates. Specifically, the presence or absence of an electron on one or more of the iron–sulfur clusters is proposed to bias the pathway of the $P700^+ A_1^-$ recombination, either via direct repopulation of the ground state of P700 or by an indirect, thermally assisted pathway which populates the putative P700 triplet. The presence of the local electric field associated with the reduced photosystem I acceptor(s) is suggested to induce a lowering of the midpoint potential for the A_1/A_1^- couple, thereby decreasing the free-energy difference between the states $P700^+A_0^-A_1$ and $P700^+A_0A_1^-$. If in analogy to the *Rhodobacter sphaeroides* reaction center the P700 triplet is populated solely via the $P700^+A_0^-A_1$

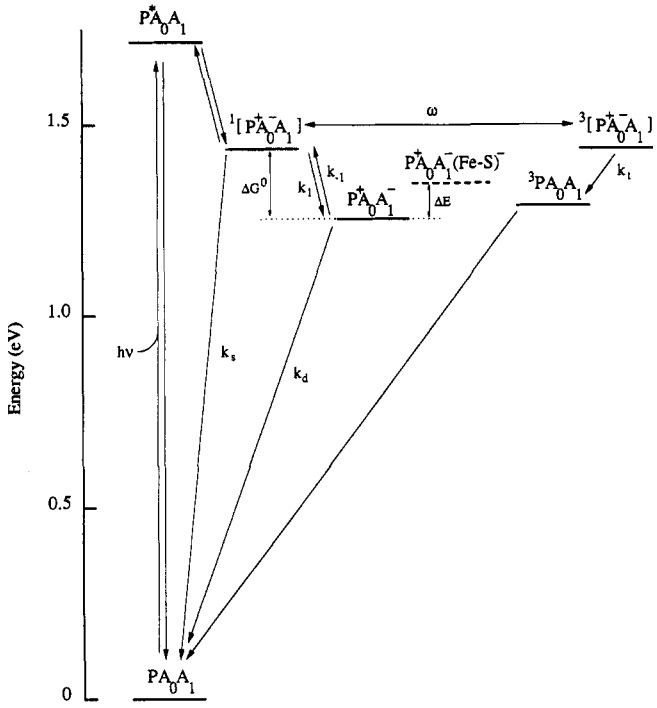

FIGURE 6: Hypothetical energy level diagram for electron transfers in the photosystem I reaction center. Intersystem crossing from the primary, singlet-correlated radical pair $^1[P^+A_0^-A_1]$ to the triplet radical pair $^3[P^+A_0^-A_1]$ is represented by the rate constant ω, and k_s and k_t are the rate constants for population of the ground and triplet states of P700. The direct pathway for charge recombination from the state $P^+A_0A_1^-$ is measured by rate constant k_d. The state $P^+A_0A_1^-(Fe\text{–}S)^-$ denotes the state $P^+A_0A_1^-$ formed in the presence of reduced iron–sulfur cluster(s).

intermediate state, then an electrostatically induced increase in the free energy of the $P700^+A_0A_1^-$ state is predicted to yield an increased lifetime for the $P700^+A_0^-A_1$ state, with a concomitant increase in triplet yield and a decrease in yield for the $P700^+A_0A_1^-$ state. Thus, the presence of the reduced iron–sulfur clusters facilitates charge recombination via the indirect pathway, whereas in the absence of the clusters recombination via the direct pathway will dominate. According to this model the A_1 acceptor is situated in closer proximity to the iron–sulfur clusters than A_0 and is thus more strongly influenced by the local electrostatic field. Hence, the free energy of the $P700^+A_0^-A_1$ state is expected to be influenced minimally by the reduced clusters.

A hypothetical energy level diagram for photosystem I electron transfers is presented in Figure 6. As proposed above, the recombination of $P700^+A_0A_1^-$ can proceed either directly with a rate constant of k_d of 10^5 s^{-1} or indirectly via thermal activation mediated by the state $P700^+A_0^-A_1$. The relative rates of recombination via these pathways will be determined by the free-energy difference between the states $P700^+A_0^-A_1$ and $P700^+A_0A_1^-$. In the absence of the (reduced) iron–sulfur clusters, we suggest that the free-energy span between these states is sufficiently large to ensure that the direct decay pathway dominates. However, in the presence of the electrostatic field contributed by the reduced acceptor cluster(s), the free-energy gap decreases to the extent that the indirect pathway dominates with kinetics distinguished by a 250-ns component. The indirect pathway is represented by the rate constant k_{id}, which is a composite of the kinetic constants k_{-1}, ω, and k_d. The recombination rate constant for the indirect pathway ($k_{id} \sim 4.0 \times 10^6$) is proposed to reflect the rate-limiting reverse electron transfer from $P700^+A_0A_1^-$ to $P700^+A_0^-A_1$, since triplet formation from the $P700^+A_0^-$ pair occurs within ca. 20 ns.

To estimate the magnitude of the free-energy gap $\Delta G°$ that would favor decay via the indirect pathway, we have utilized a formulism analogous to that of Gopher et al. (1985), that is, solving for the $\Delta G°$ that would effect equivalent recombination rates for the direct and indirect pathways.

$$\Delta G°' = k_b T \ln (k_{id}/k_d)$$

With the appropriate substitutions ($k_d = 10^5$ s^{-1}, $k_{id} = 4.0 \times 10^6$ s^{-1}, $T = 293$ K, and $k_b = 86 \times 10^{-6}$ ev/K), $\Delta G°'$ is calculated to be ca. 93 mV. This value, when compared to the estimated free-energy gap of ca. 250 mV between $P700^+A_0^-A_1$ and $P700^+A_0A_1^-$ in the absence of reduced secondary acceptors, suggests that the electrostatic contribution from the iron–sulfur centers results in a decrease of the free-energy gap in excess of 150 mV. Similar calculations, presupposing a quasi-equilibrium involving the states $P700^+A_0^-A_1$ and $P700^+A_0A_1^-$, predict that in the absence of the reduced centers ($\Delta G° \sim$ 250 mV) that ca. 98% of the backreaction occurs through the direct pathway; however, under the influence of the electrostatic contribution from the reduced iron–sulfur cluster(s), greater than 90% of the reaction centers are expected to recombine by the direct pathway.

Although electrostatic control of electron-transfer kinetics in photosynthesis has been postulated previously (Brettel et al., 1984; Sétif & Mathis, 1986; Golbeck & Cornelius, 1986), the literature is devoid of unambiguous supporting data. Thus, the recent study by Serr et al. (1988) of the electrochemistry of a triply bridged, dinculear iron complex is particularly germane. The authors report a substantial interaction between the iron centers, an interaction that is manifested by shifts in reduction potentials and is electrostatic in origin. Applying a simple electrostatic theory gave a qualitative agreement between the magnitude of interaction and the distance between the electroactive species. These observations are significant and provide for the first time an experimental precedence for application to biological electron transport. In this regard, a similar electrostatic model can be applied to the photosystem I reaction center, with the energy of interaction represented by

$$\Delta E = [(e^2)/4\pi\epsilon_0\epsilon_r](1/r)$$

Evaluation of this expression involves two assumptions: (1) the electrons are localized (i.e., point charges) and (2) the dielectric constant of the reaction-center protein medium (ϵ_r) is continuous and uniform with an estimated value of 4. If the distance of separation between the charges (r) is set at 10 Å, a value not incongruous with the postulated separation of A_1 and F_X, then the interaction energy is calculated to effect a decrease of the midpoint potential for the A_1/A_1^- couple of 350 mV. Given the limiting assumptions, this crude calculation is consistent qualitatively with the premise that the electrostatics of the acceptor complex in photosystem I can determine the recombination pathway.

The acceleration in the $P700^+$ A_1^- backreaction from 10 μs in the absence of the iron–sulfur clusters to 250 ns in the presence of F_X^-, F_B^-, and F_A^- is regarded therefore as a consequence of the presence of a charged component in close proximity to A_1^-. The latter is not considered a physiologically relevant state because the iron–sulfur clusters are probably only rarely fully reduced in the working thylakoid membrane. The extremely high quantum yield for stable charge separation between P700 and F_A/F_B (Owens et al., 1990) requires that forward transfer time at each acceptor be typically 2–3 orders

of magnitude greater than the corresponding backreaction of that acceptor with $P700^+$. Accordingly, the 4–15-ns forward electron transfer time [200 ns in Brettel (1988)] from A_1^- to F_X (Mathis & Sétif, 1988; Warden, 1989) would have a more difficult time outcompeting a 250-ns backreaction (found in the presence of reduced F_X^-, F_B^-, and F_A^-) than a 10-μs backreaction (found in the absence of F_X, F_B, and F_A). On the basis of this reasoning, the inherent half-time for the $P700^+$ A_1^- charge recombination in *Synechococcus* sp. PCC 6301 in the presence of oxidized F_X, F_B, and F_A is probably closer to 10 μs than 250 ns.

REFERENCES

Biggins, J., & Mathis, P. (1988) *Biochemistry 27*, 1494–1500.

Bottin, H., Sétif, P., & Mathis, P. (1987) *Biochim. Biophys. Acta 894*, 39–48.

Brettel, K. (1988) *FEBS Lett. 239*, 93–98.

Brettel, K. (1989) *Biochim. Biophys. Acta 976*, 246–249.

Brettel, K., & Sétif, P. (1987) *Biochim. Biophys. Acta 893*, 109–114.

Brettel, K., Schlodder, E., & Witt, H. T. (1984) *Biochim. Biophys. Acta 766*, 403–415.

Brettel, K., Sétif, P., & Mathis, P. (1986) *FEBS Lett. 203*, 220–224.

den Blanken, H. J., & Hoff, A. J. (1983) *Biochim. Biophys. Acta 724*, 52–61.

Golbeck, J. H., & Cornelius, J. M. (1986) *Biochim. Biophys. Acta 849*, 16–24.

Gopher, A., Blatt, M., Schönfeld, M., Okamura, M., Feher, G., & Montal, M. (1985) *Biophys. J. 48*, 311–320.

Hoshina, S., Sakurai, R., Kunishima, N., Wada, K., & Itoh, S. (1990) *Biochim. Biophys. Acta 1015*, 61–68.

Hurley, J. K., Castelli, F., & Tollin, G. (1980) *Photochem. Photobiol. 32*, 79–86.

Ikegami, I., Sétif, P., & Mathis, P. (1987) *Biochim. Biophys. Acta 894*, 414–422.

Itoh, S., Iwaki, M., & Ikegami, I. (1987) *Biochim. Biophys. Acta 893*, 508–516.

Li, N., Zhao, J. D., Warren, P. V., Warden, J. T., J., Bryant, D., & Golbeck, J. H. (1991) *Biochemistry 30*, 7863–7872.

Mathis, P., & Sétif, P. (1981) *Isr. J. Chem. 21*, 316–320.

Mathis, P., & Sétif, P. (1988) *FEBS Lett. 237*, 65–68.

Mathis, P., Ikegami, I., & Sétif, P. (1988) *Photosynth. Res. 16*, 203–210.

McDermott, A. E., Yachandra, V. K., Guiles, R. D., Sauer, K., Parrett, K. G., & Golbeck, J. H. (1989) *Biochemistry 28*, 8056–8059.

Mehari, T., Parrett, K. G., Warren, P. V., & Golbeck, J. H. (1991) *Biochim. Biophys. Acta 1056*, 139–148.

Owens, T. G., Carpentier, R., & Leblanc, R. M. (1990) *Photosynth. Res. 24*, 201–208.

Parrett, K. G., Mehari, T., Warren, P. V., & Golbeck, J. H. (1989) *Biochim. Biophys. Acta 973*, 324–332.

Parrett, K. G., Mehari, T., & Golbeck, J. H. (1990) *Biochim. Biophys. Acta 1015*, 341–352.

Petrouleas, V., Brand, J. J., Parrett, K. P., & Golbeck, J. H. (1989) *Biochemistry 28*, 8980–8983.

Sauer, K., Mathis, P., Acker, S., & Van Best, J. A. (1979) *Biochim. Biophys. Acta 545*, 466–472.

Schroeder, H.-U., & Lockau, W. (1986) *FEBS Lett. 199*, 23–27.

Serr, B. R., Anderson, K. A., Elliott, C. M., & Anderson, O. P. (1988) *Inorg. Chem. 27*, 4499–4504.

Sétif, P., & Bottin, H. (1989) *Biochemistry 28*, 2689–2697.

Sétif, P., & Brettel, K. (1990) *Biochim. Biophys. Acta 1020*, 232–238.

Sétif, P., & Mathis, P. (1986) *Photosynth. Res. 9*, 47–54.

Sétif, P., Quaegebeur, J. P., & Mathis, P. (1982) *Biochim. Biophys. Acta 681*, 345–353.

Sétif, P., Bottin, H., & Mathis, P. (1985) *Biochim. Biophys. Acta 808*, 112–122.

Sétif, P., Ikegami, I., & Biggins, J. (1987) *Biochim. Biophys. Acta 894*, 146–156.

Strain, H. H., & Svec, W. A. (1966) in *The Chlorophylls* (Vernon, L. P., & Seely, G. R., Eds.) pp 21–66, Academic Press, New York.

Warden, J. T. (1989) in *Current Research In Photosynthesis* (Baltscheffshy, M., Ed.) Vol. 2, pp 635–638, Kluwer, Dordrecht.

Warden, J. T., & Golbeck, J. H. (1987) *Biochim. Biophys. Acta 891*, 286–292.

Warren, P. V., Parrett, K. G., Warden, J. T., & Golbeck, J. H. (1990) *Biochemistry 29*, 6545–6550.

Zhao, J., Warren, P. V., Li, N., Bryant, D. A., & Golbeck, J. H. (1990) *FEBS Lett. 276*, 175–180.